PERFORMANCE OF A PASSIVE ACOUSIC LINEAR ARRAY IN A TIDAL CHANNEL

David R. Barclay [a], Matthew F. Auvinen [a]

[a] Department of Oceanography, Dalhousie University, 1355 Oxford Street, Halifax, NS B3H4R2 Canada

David Barclay
Dalhousie University
1355 Oxford Street
Halifax, NS B3H4R2 Canada
FAX: 902-494-3877

Abstract: *Baseline ambient sound level assessment is important in quantifying noise contributions from tidal energy infrastructure. Static acoustic sensing in high-flow conditions is complicated by pseudo-sound, or flow noise, generated by pressure fluctuations due to turbulent flow on the surface of a hydrophone. Signal processing methods are used to identify and suppress flow noise at low frequencies (< 500 Hz) in data collected on a four element horizontal hydrophone array in the Minas Passage, a tidal channel in the Bay of Fundy, in October 2016. Spectral slope analysis is used to identify the spectral critical frequency, where the flow noise and ambient noise contributions to the recorded signal are equal. Spatial coherence analysis is to identify the coherence critical frequency, where the first instance of flow noise occurs. The array's performance in the Minas passage is quantified by an empirical relationship between flow speed and the spectral critical frequencies of the coherent output from the liner array. Coherent averaging (broadside beamforming) is demonstrated as an effective flow noise suppression technique, improving low-frequency passive acoustic monitoring in a high energy tidal channel.*

Keywords: *Flow noise, ambient noise, acoustical array, tidal channel, and passive acoustic monitoring*

1. INTRODUCTION

Tidal power utilities are currently leasing seafloor space within the Minas Passage in the Bay of Fundy with aspirations of converting the energy of the region's tidal currents into electricity, a trend that has been supported by favourable projections of the Passage's tidal energy capacity [1]. Stakeholders, regulators, and tidal power companies are interested in establishing baseline ambient noise measurements in the Minas Passage, against which turbine noise pollution will be measured. However, the utility of ambient sensing is limited by pseudo-sound, or flow noise, generated on the surface of a hydrophone in turbulent water. The objectives of the present research are: (1) Use spectral analysis and spatial coherence to identify and characterize flow noise at low frequencies (< 500 Hz) and (2) use coherent averaging (beamforming) to improve the performance of a linear hydrophone array by suppressing flow noise and enhancing the measurement of ambient noise.

2. FIELD WORK

Field work was completed on October 27, 2016, near the Fundy Ocean Research Center for Energy (FORCE) site in the Minas Passage of the Bay of Fundy. The deployment period spanned roughly four hours, from 12:00 ADT to 16:00 ADT. This experimental window captured the transition from ebb tide to slack tide.

A linear hydrophone array was streamed behind the *MV Nova Endeavour*, which was anchored to the seafloor in the Minas Passage. The array was positioned 15 meters below the sea surface using a depressor. Four hydrophones were simultaneously sampled over a four hour period and processed by an analog-to-digital converter (ADC) on board the *MV Nova Endeavour*. The linear array was constructed by GeoSpectrum Technologies, and contains four sequentially spaced hydrophones with a horizontal configuration. Each hydrophone pair is separated by a distance d = 17 cm. The array hydrophones were set to simultaneously sample at a rate of 96.038 kHz with an acoustic bandwidth of 48.019 kHz.

A drifting hydrophone (Geospectrum Technologies GuardBuoy) was deployed using a small auxiliary vessel launched from the *MV Nova Endeavour*. The GuardBuoy was suspended 2 meters below the surface using a drifting surface float and isolation system made of spectra and compliant bungee. The GuardBuoy sampled at a rate of 96 kHz with an acoustic bandwidth of 48 kHz, and was equipped with a GPS to record transect geospatial information.

A total of five transects were performed by driving the GuardBuoy upstream, deploying the drifter, then floating downstream in a rigid-hulled inflatable boat (RHIB) alongside the GuardBuoy. The GuardBuoy and RHIB followed a transect that passed over the array and then an additional 20 meters.

The Guard Buoy signals are assumed to be flow noise free and were used as benchmarks to assess the performance of the array. The turbulent tidal channel is assumed to be well mixed with an isovelocity sound speed profile, minimizing noise field variability over the depth difference between the two systems.

3. DATA ANALYSIS

The output of a hydrophone is defined as

$$x_i(t) = \sigma_i(t) + n_i(t) \tag{1}$$

where x_i is the recorded time series on each ith hydrophone, σ_i is the sound field's ambient components, and n_i is the locally generated flow noise. Importantly, n_i and σ_i are uncorrelated. Furthermore, the inherent randomness of flow noise makes n_i incoherent with respect to n_j.

The power spectrum, or spectral density, is defined as

$$S_{ii}(\omega) = \frac{\left\langle X_i(\omega) \cdot X_i^*(\omega) \right\rangle}{T} \tag{2}$$

where X_i is the Fourier transform of x_i, ω is angular frequency, * denotes a complex conjugate, < > indicates an ensemble average, and T is the observation interval. All Fourier transforms are windowed by a Hann function. The Fourier transform is 2^{16} points long and contains 99 degrees of freedom.

Locally generated flow noise and the ambient sound field are inseparable, however we can describe their relative prevalence with the theoretical signal-noise ratio (SNR) where we are defining ambient sound as the signal, and flow noise as the noise. By taking the Fourier transform of (1) and substituting into (2), we find the SNR for a single hydrophone (SNR_H):

$$SNR_H = \frac{\left\langle \varsigma_i \varsigma_i^* \right\rangle}{\left\langle N_i N_i^* \right\rangle}. \tag{4}$$

We use a broadside beamformer to coherently average the channels across the array such that the SNR for the coherent array (SNR_A) is

$$SNR_A = \frac{K\left\langle \varsigma_i \varsigma_i^* \right\rangle}{l\left\langle N_i N_i^* \right\rangle} \tag{5}$$

where

$$K = l + \sum_{i=1}^{l-1} (l-i)\cos(\omega \tau_i) \tag{6}$$

and

$$\tau_i = \frac{i \cdot d \cos\theta}{c} \tag{7}$$

Where l is the number of elements across the array, d is the nearest neighbour element separation, and c is the sound speed. Comparing (5) to the result derived for a single hydrophone, given by (4), we see that the beamformed array improves the signal-to-noise ratio by a factor of K/l. Furthermore, (5) indicates that array performance improves with an increasing number of hydrophones, l. For an array with 4 elements, at broadside, $K/l = 7/4$.

The broadside beamforming analysis applied to the linear array generates artificial spectral density gain. As a result, an array gain formula is applied to the beamformed results to correct the inflated values. The array gain formula presented here is adapted from Cox [2], such that

$$AG = 20\log l \tag{8}$$

4. RESULTS

Signal levels (Fig. 1) are relatively high in fast flowing water and low in slow flowing water. The mid-to-high-frequency band is less affected by flow noise and is quiet relative to lower frequencies (< 10 Hz). Evidently, flow noise is prevalent below 100 Hz. The wind speed varied between 3.2 and 6.2 m/s with a mean of 5.0 m/s. The hydrophone power spectrum contains multiple episodes of mid-frequency noise. These signals are attributed to ship noise generated by the small vessel used in the GuardBuoy drifter tests. Additionally, the abrupt shift in spectral density at 90 minutes is due to equipment reconfigurations.

The PSPD facilitates the broad-scale assessment of a hydrophone's spectral density over entire deployment periods. The PSPD for each hydrophone on the array are constructed by compiling histograms across the entire deployment period.

The PSPD follows a spectral slope of $f^{-5/3}$ below 10 Hz, behaviour analogous to Kolmogorov's turbulence theory. A steepened spectral slope of f^{-m}, where $m > 5/3$, persists between 10 and 100 Hz, a result of small-scale turbulence. The PSPD results show that ambient noise is dominant above 300 Hz, where signal levels are markedly low. An electronic system noise floor persisted at about 60 dB re µPa throughout the deployment.

We define the spectral critical frequency as the frequency at which the flow noise and ambient noise contributions to the recorded signal are equal in power. As such, the spectral critical frequency marks the transition from the flow noise region to the ambient noise region in Fig. 2. Below the spectral critical frequency flow noise signal contamination is severe and above the spectral critical frequency the signal is composed of a mixture of both flow and ambient noise.

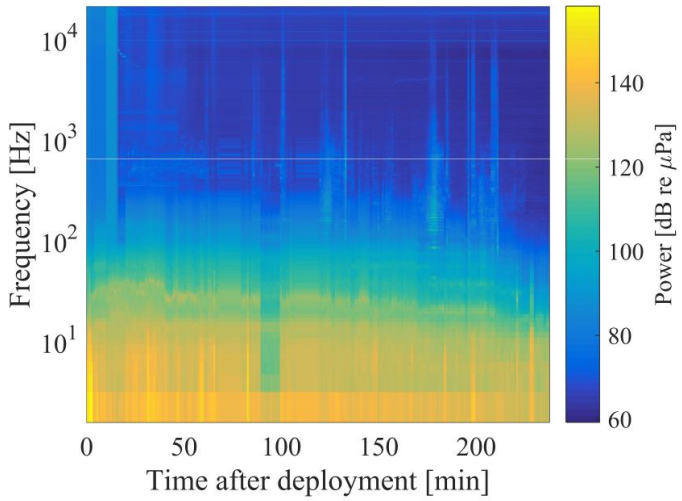

Fig 1: Power spectrum for channel 0 on the array. The spectrum is plotted over the deployment period across a range of low-to-mid frequencies. The spectrum begins at maximum ebb tide and ends shortly after slack tide, as shown by the current speed time series. Power decreases with current speed over the deployment period.

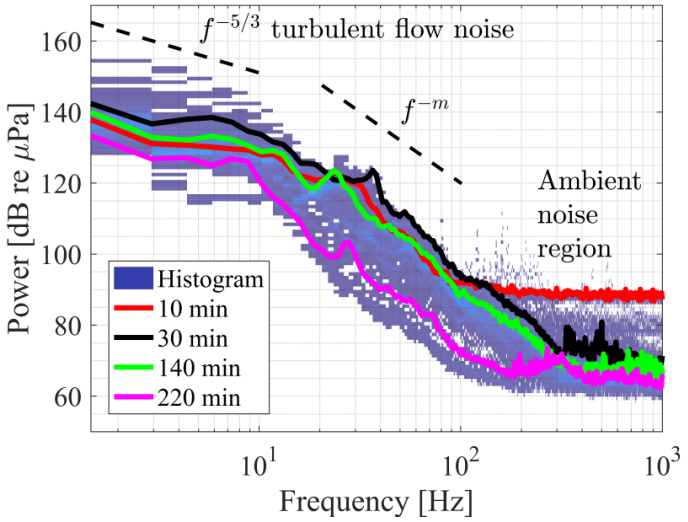

Fig 2: Fixed single hydrophone power spectrum probability density over the entire deployment period. Turbulent flow noise is prevalent < 10 Hz (where wavelengths >> sensor size), with a spectral slope of $f^{-5/3}$, while turbulence interacting with the hydrophone's finite volume (in the 10 Hz to 100 Hz band) yields a spectral slope of f^{-m}. The ambient sound field dominates at frequencies > 300 Hz. Coloured lines represent individual spectra recorded at the time after deployment indicated in the legend.

Flow noise is uncorrelated and propagating ambient noise is highly correlated at low frequencies. Therefore, the spatial coherence results (Fig. 3) are partitioned into two distinct

regions: a flow noise region and an ambient noise region. Visual assessment suggests that flow noise is consistently present at low frequencies and can be prominent at higher frequencies (> 600 Hz). Such coherence boundaries are the basis of the coherence critical frequency, which is the highest frequency at which flow noise can be detected.

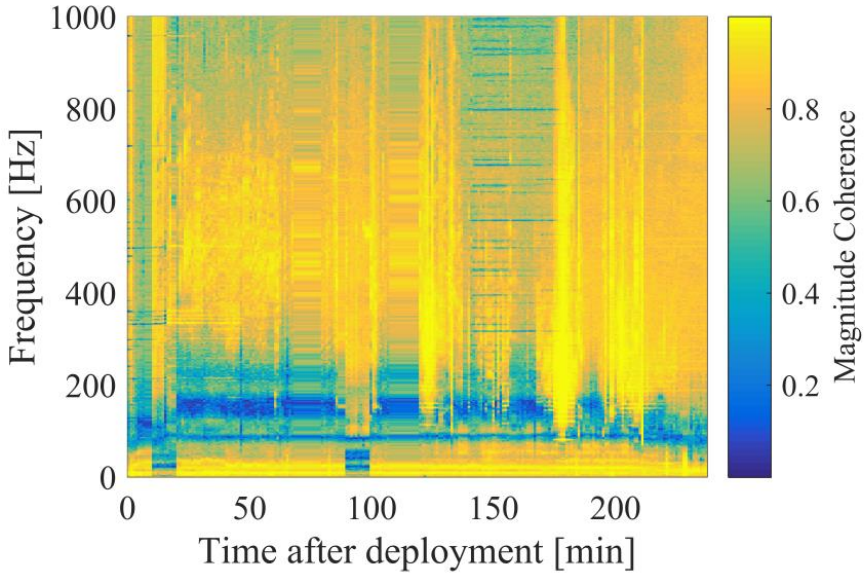

Fig. 3: Spatial coherence over the experimental period. Magnitude coherence is expected to tend to unity as the fixed hydrophones become relatively co-located. However, uncorrelated flow noise on each phone breaks that relationship. The extent of incoherent flow noise increases with current speed. Channel 0 - 1 (a) and 0 - 3 (b) are shown as examples. Results hold to all other channel combinations.

The spectral critical frequency of the coherent array output is compared to the fixed single hydrophone spectral and coherence critical frequencies in Fig. 4. The standard deviations of the spectral slope and spatial coherence critical frequency regressions were extracted from the averaged fits, while the standard deviation of the coherent array critical frequency regression was calculated from the data during the regression.

The coherence critical frequencies are relatively high, while spectral critical frequencies (both fixed single hydrophone and coherent array) are relatively low. This is attributed to the more sensitive nature of the coherence-based method. Above coherence critical frequencies we can be confident that there is no contamination of the ambient noise field by flow noise. Conversely, the fixed single hydrophone and coherent array spectral critical frequencies show where flow noise and ambient noise have equal power. The coherence and spectral critical frequencies serve as the respective upper and lower bounds of different noise regimes. Importantly, the coherent array output contains significantly lower critical frequencies than the fixed single hydrophone, indicating that the broadside beamforming approach lessens the extent of flow noise within the measurements.

Fig. 5 illustrates the relationship between spectral critical frequency and the number of hydrophone elements on an array across a range of current speeds. We observe an inverse relationship between spectral critical frequency and hydrophone count.

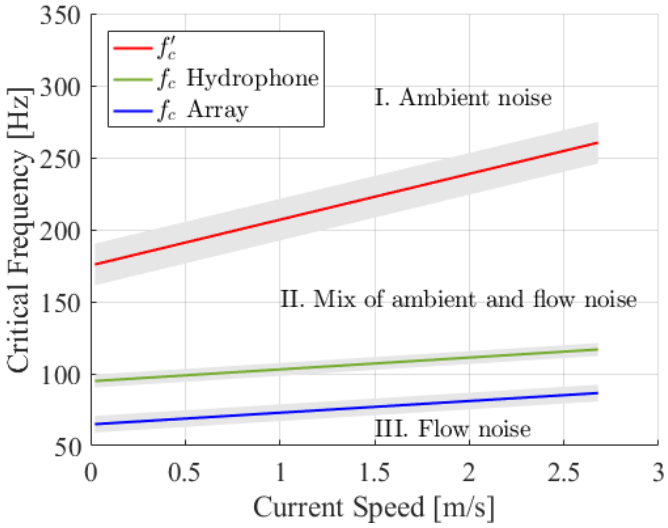

Fig. 4: Comparison of fixed single hydrophone spectral critical frequency (green), array spectral critical frequency (blue), and coherence critical frequency (red) as a function of current speed. Uncertainties are one standard deviation (shaded). Coherence critical frequency, f'_c, separates region I, where flow noise is negligible, and region II, where flow and ambient noise are both present, while spectral critical frequency, f_c separates regions II and III, where flow noise dominates. The coherent array effectively suppresses flow noise, as indicated by its lower boundary relative to the fixed single hydrophone.

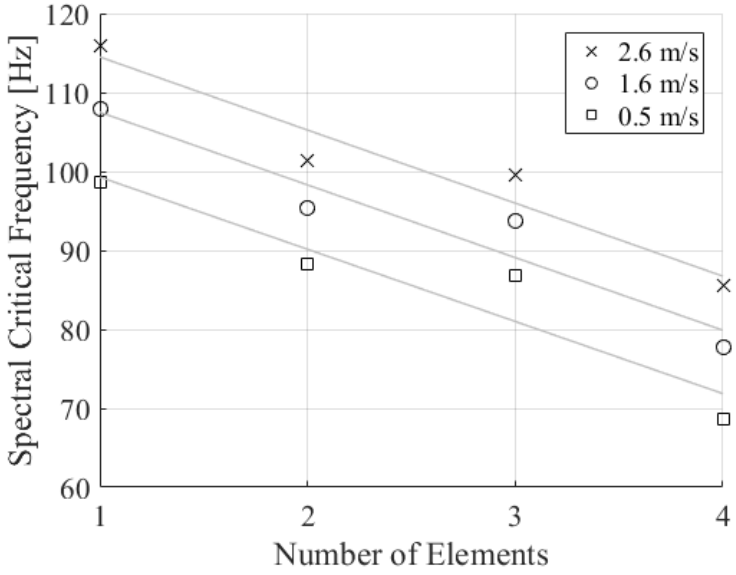

Fig. 5: Relationship between spectral critical frequency and the number of elements on an array across a range of current speeds. There is a sequential relationship, where f_c is lowered as more hydrophones are added to the array.

REFERENCES

[1] **R. Karsten, A. Swan, and J. Culina,** "Assessment of arrays of in-stream tidal turbines in the Bay of Fundy," *Phil. Trans. R. Soc. A*, 306 vol. 371, no. 1985, p. 20120189, 2013.

[2] **H. Cox,** "Line array performance when the signal coherence is spatially dependent," *The Journal Of The Acoustical Society Of America*, vol. 54, no. 6, pp. 1743–1746, 1973.